COMPARISON BETWEEN AN ALLISON SCANNER AND THE KVI-4D EMITTANCE METER*

H. R. Kremers#, J. P. M. Beijers, S. Brandenburg, S. Saminathan, V. Mironov, Kernfysisch Versneller Instituut, University of Groningen , Groningen, the Netherlands
T. Thuillier, LPSC, CNRS/IN2P3, UJF, INPG, Grenoble, France.

INTRODUCTION

The demand for intense highly-charged ion beams at the AGOR facility has triggered a study to improve the beam-line transport efficiency. In the framework of this study an emittance meter (KVI-4D) to measure the 4D phase-space of a beam has been developed. The device is also intended for use at GSI with the MS-ECRIS, which is being built in the framework of the EURONS-ISIBHI project.

The demand for intense beams is pushing the development of ECR ion sources to areas where the formation of ion beams in the extraction region is affected by the strong fringe field of the solenoids and extracted intense beams are influenced by space charge effects. With the KVI-4D emittance meter we hope to gain more understanding of beam formation and transport and thus to improve overall efficiency.

In the following we will describe the design and the main parameters characterizing the instrument. Measurements will be presented where we compare data taken with an Allison [1] scanner and with the KVI-4D [2] emittance meter for the same beam. An exploration of the 4D phase-space data shows how beam filamentation can be investigated.

THE MEASUREMENT CONCEPT AND MAIN CHARACTERISTICS

The emittance meter has been designed to analyze a low-energy ion beam at the image plane of an analyzing magnet. At the image plane, the beam has an estimated maximum waist of 5 mm in the horizontal direction and a beam size of 40 mm in the vertical direction. The corresponding divergences are about +/-50 mrad and +/-6 mrad respectively. The instrument is design such that it is able to accept beams with a power up to 150 W.

To measure the emittance in four dimensions the pepper pot method [3, 4] has been adopted. Implementation of this principle led to the basic design of a tantalum pepper pot plate (see Fig.1) with a thickness of 25 µm, machined with an array of 20 µm diameter holes with a pitch of 2 mm. Each hole position is accurately defined in the y-direction. The plate is mounted at a distance of 59.3 mm from a MCP-based position-sensitive detector which has been described in [2]. The pepper pot plate is stepped with a translation device in the x-direction through the beam. The accuracy of this movement is less than a micrometer. Images are recorded at each step and contain a row of spots in the y-direction. Each spot covers 500-3000 pixels of the CCD. Each pixel is defined accurately in a second coordinate system. By scanning a single row of holes over the beam area, overlap of the spots in the x-direction, where the divergence is large, is impossible. In the y-direction the divergence is much smaller, so that no overlap occurs for the 2 mm hole pitch, small compared to the 40 mm beam size.

From the measured positions of the ions and the exact position of the pepper pot plate we can reconstruct the rectilinear flight path of the particles and thus also the angular coordinates x’ and y’. A 4D dataset $\rho(x,y,x',y')$ can be constructed that contains an intensity value proportional to the number of detected particles within a 4D volume-element dx, dy, dx’, dy’ at the phase-space position x, y, x’, y’.

The dataset ρ can now be used to construct the various phasespace projections: x-x’ (see Eq.1); y-y’ and also x-y’, y-x’ by integrating over the other dimensions.

$$\rho(x,x') = \iint \rho(x,y,x',y')dydy' \quad (1)$$

By integrating over specific intervals of the other dimensions more detailed information can be obtained. An example of this will be discussed below.

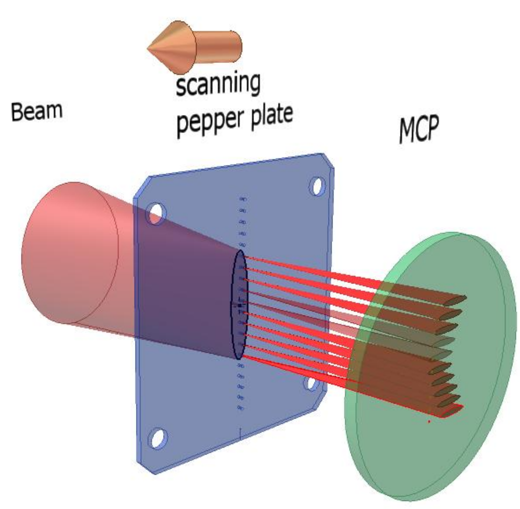

Figure 1: measurement concept of the KVI-4D emittance meter

* This work has been supported by the University of Groningen and by the European Union through EURONS, contract 506065. It has been performed as part of the research programme of the "Stichting voor Fundamenteel Onderzoek der Materie" (FOM), with support of the "Nederlandse Organisatie voor Wetenschappelijk Onderzoek" (NWO).

#kremers@kvi.nl

To be able to measure intense beams we need to reduce the beam power on the MCP surface as it is sensitive to sputtering effects. Here, the pepper pot principle has a clear advantage. It stops essentially the whole beam and the transmitted beamlets formed by the holes have a much lower power density because of their divergence. In our case the power density is reduced with a factor of $3x10^{-4}$. So a power deposition of 20 W/ cm^2 on the pepper pot plate results in a power deposition of 6 mW/cm^2 at the MCP surface. This decrease in power deposition makes it possible to measure intense low energy beams.

To optimize this reduction the hole diameter is minimized. To keep a large instrumental acceptance with respect to the beam emittance the thickness of the pepper pot plate needs to be reduced too. This decreases the heat conduction through the pepper pot plate material. Taking this into consideration in combination with the sputtering yields of a 150W beam on the tantalum pepper pot plate, a lower limit of the hole diameter is reached in the order of 5-10 µm.

DATA ANALYSIS

The dataset ρ(x, y, x', y') contains an intensity value obtained from a single pixel of the CCD camera and contains background, noise and beam related signal. The background and noise originate in both the MCP and CCD. The background is eliminated by subtracting an image taken without beam from the data. In order to determine the noise threshold the frequency distribution of the content of the pixels is constructed. The distribution (see Fig. 2) consists out of a bell shape part due to the noise and the tail part related to the beam. The threshold to separate the noise from the beam related signal is set by the 3 sigma of the Gaussian fit.

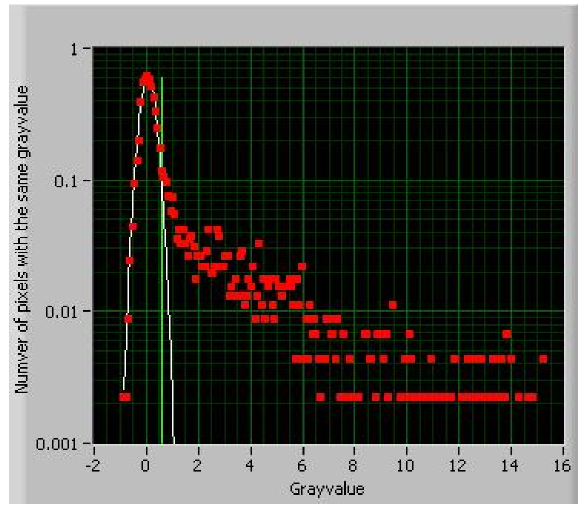

Figure 2: Frequency distribution of the dataset, white: Gaussian fit, green: 3 sigma threshold

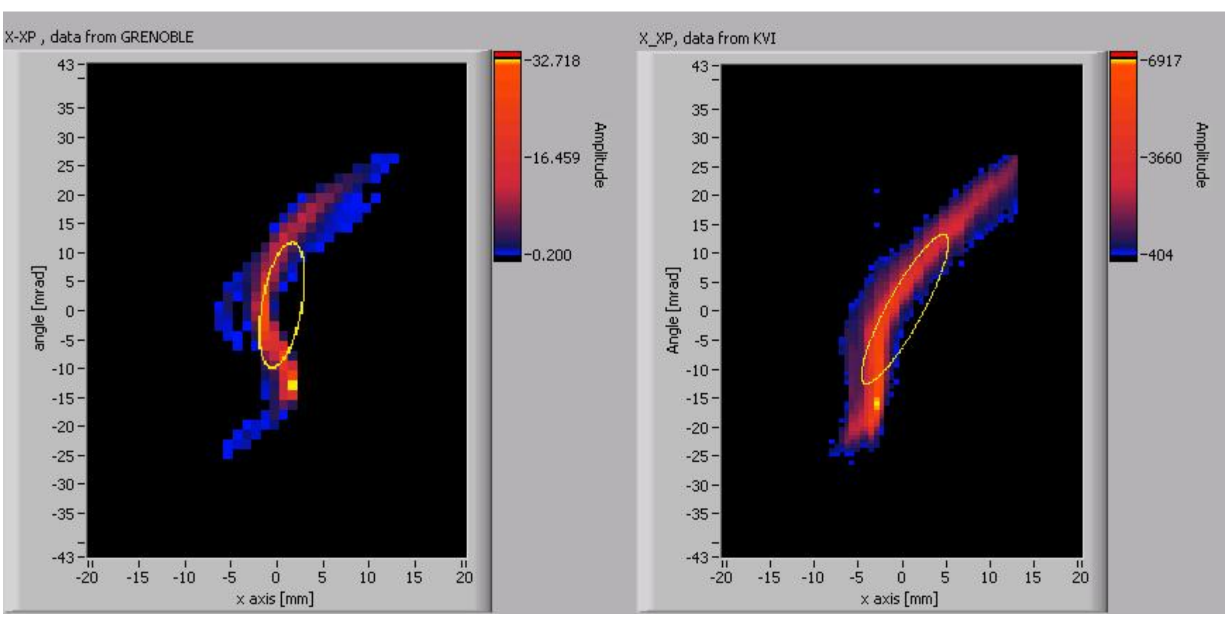

Figure 3: X-x' emittance measured with the KVI-4D emittance meter and the Allison scanner, both fitted with a 1σ RMS ellipse fit.

The beam related signal is used to calculate a RMS emittance [5]. The routine calculates the centre, the variance in both directions and plots the ellipse in an x-x' or y-y' coordinate system. The ellipse contains 68% of the intensity. To compare the outcome of the KVI-4D emittance meter with the 2D Allison scanner integration over the full dataset is needed

COMPARISON OF THE INSTRUMENTS

The KVI-4D emittance meter was installed 30 cm downstream a set of two Allison scanners at the test bench of A-Phoenix at LPSC Grenoble [6]. The emittance was measured with both devices subsequently. Measurements were made for different charge states and intensities of a Ne-beam at an extraction voltage of 35 kV. The influence of the MCP-gain on the measurements was also investigated. The data was analyzed with the above described RMS-fit routine.

From table 1, one can observe that with the Allison scanner a normalized emittance of 0.14 +/- 0.02 π mmmrad for the charge state 4+ has been found. With the KVI-4D emittance meter a value of 0.16+/-0.01 π mmmrad is obtained. So we conclude that the measurements with both instruments are consistent (see Fig. 3). The small effect of the increase of the RMS-emittance as a function of the MCP-gain will be investigated further.

Table 1: Normalized RMS emittance (1σ) as function of the charge, beam current, and high voltage on the MCP.

no	E	Beam cur	Charge	HV MCP	KVI-4D x-x'	Allison x-x'
	keV	μA			π [mmmrad]	π [mmmrad]
A41	140	500	4+	5.1	0.17	0.15
A42	140	500	4+	4.8	0.16	
A43	140	500	4+	4.6	0.15	
A51	120	500	4+	5.2	0.16	0.13
A52	120	500	4+	4.9	0.15	
A61	210	180	6+	5.3	0.16	0.18
A62	210	200	6+	4.7	0.14	
A71	280	18	8+	5.7	0.19	0.13
A72	280	18	8+	5.1	0.16	

X – Y CORRELATIONS

The KVI-4D emittance meter measures the full four dimensional transverse phasespace density of the beam, thus allowing the analysis of correlations between the two transverse planes x-x' and y-y'. As an example of such an analysis we show in Fig. 4 the phasespace distribution ρ(x,x') extracted from the KVI-4D measurement shown in Fig. 3, by integrating over the full y-dimension and the interval -13<y'<-11 mrad. The phasespace distribution exhibits two more or less separated S-like structure. We observe that at certain angles y', the beam in the x-x' plane is split into two parts with similar focussing properties.

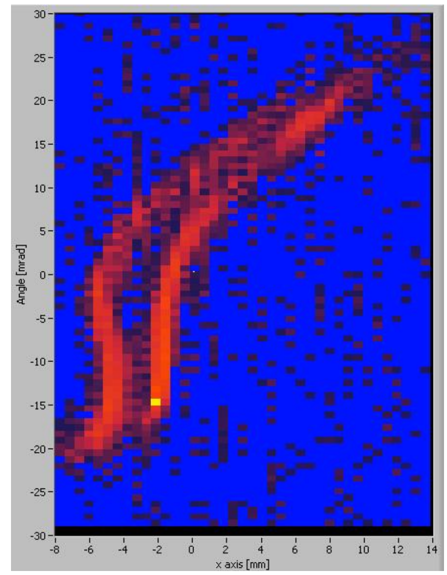

Figure 4: KVI-4D emittance x-x'(-20<y<20mm, -13<y'<-11 mrad)

Further analysis of the data shows that the left S-structure originates from the upper half of the beam, while the right S-structure originates from the lower half of the beam as can be seen from Fig.5. This illustrates how 2D-projections of the phasespace distribution obtained by integrating over a part of the full range for the orthogonal dimensions gives a more detailed insight in the structure of the phase space distribution.

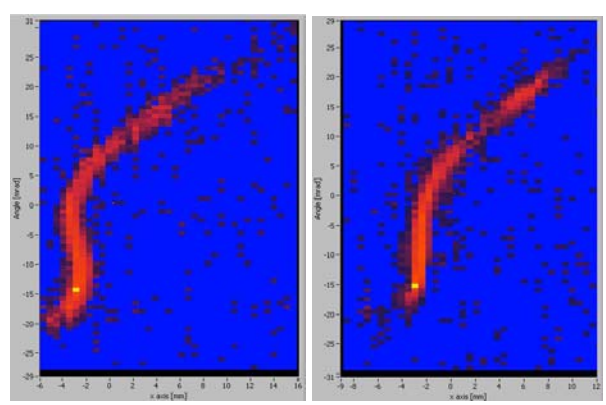

a) b)

Figure 5: KVI-4D, x-x' a)0<y<20, -13<y'<-11mrad, b)-20<y< 0, -13<y'<-11mrad

CONCLUSION

An instrument was developed to measure the full four dimensional phasespace distribution of low-energy highly-charged heavy ion beams. We have shown earlier [2] that it operates in a mode where we can detect single ions as well as with a beam current of 500 μA (20W) without damaging the detector. This is basically due to the dynamical range of the gain of the MCP. The emittances measured with the Allison scanner and the KVI-4D meter of the same beam are consistent with each other. Correlations between the transverse planes can be measured in detail. The complete 4D-structure of the phasespace distribution will help improving the understanding of beam formation and extraction in ECR-sources and in obtaining an optimum transport and matching of the beam to the accelerator.

REFERENCES

[1] P.W. Allison, J. D. Sherman, and D. B. Holtkamp, *IEEE Trans. Nucl. Sci.* **NS-30**, 2204-2206 (1983).

[2] H. R. Kremers, J. P. M. Beijers, S. Brandeburg, DIPAC'07, Venice, May 2007, TUPC24, (2007).

[3] L.E. Collins and P.T. Stroud, Nucl. Instr. and Meth. 26 (1964) 157.

[4] C. Lejeune and J. Aubert, Applied Charged Particle Optics,Ed. A. Septier (Academic Press, 1980) p. 159.

[5] J. Buon, CERN Accelerator School Proceedings (Editors : S. Turner) 94-01; vol. II p 89 (1994)

[6] T. Thuillier, T. Lamy, P. Sortais, P. Suominen, O. Tarvainen, and H. Koivisto, Rev. Sci. Instrum. 77, 03A323 (2006).